Experimental Observation of Dark Solitons on the Surface of Water

A. Chabchoub,[1,2,*] O. Kimmoun,[3] H. Branger,[4] N. Hoffmann,[1,2] D. Proment,[5] M. Onorato,[6,7] and N. Akhmediev[8]

[1]*Department of Mechanical Engineering, Imperial College London, London SW7 2AZ, United Kingdom*
[2]*Mechanics and Ocean Engineering, Hamburg University of Technology, 21073 Hamburg, Germany*
[3]*École Centrale Marseille, 13013 Marseille, France*
[4]*IRPHE, UMR 7342, CNRS, AMU Aix Marseille Université, 13013 Marseille, France*
[5]*School of Mathematics, University of East Anglia, Norwich NR4 7TJ, United Kingdom*
[6]*Dipartimento di Fisica, Università degli Studi di Torino, 10125 Torino, Italy*
[7]*Istituto Nazionale di Fisica Nucleare, INFN Sezione di Torino, 10125 Torino, Italy*
[8]*Optical Sciences Group, Research School of Physics and Engineering, Institute of Advanced Studies, The Australian National University, Canberra ACT 0200, Australia*

(Received 3 September 2012; published 21 March 2013)

We present the first ever observation of dark solitons on the surface of water. It takes the form of an amplitude drop of the carrier wave which does not change shape in propagation. The shape and width of the soliton depend on the water depth, carrier frequency, and the amplitude of the background wave. The experimental data taken in a water tank show an excellent agreement with the theory. These results may improve our understanding of the nonlinear dynamics of water waves at finite depths.

DOI: 10.1103/PhysRevLett.110.124101 PACS numbers: 05.45.Yv, 47.35.Fg, 92.10.Hm, 92.40.Qk

There is a deep analogy between waves in optics and on the surface of water. Developing this analogy allows us to conduct research in one area and expand the ideas to another one. Such an expansion has been particularly fruitful in the studies of rogue waves, which first appeared from the gossip of seafarers before finding solid ground as objects of research in oceanography [1], then later in optics [2], and now the new concept is widely used in many other fields of physics [3]. Unifying ideas [3] help to establish common ground in this exciting area of research.

There is one particular type of nonlinear waves previously studied in optics and plasma physics which until now has not been observed in the case of water waves. As a result, we cannot estimate the importance of these waves in natural phenomena although they can surely be present among the variety of ocean waves destructively acting along the shores: tsunamis, seiches, bores, tidal waves, etc. This special wave is commonly known as a dark soliton. In optics, this wave can be described as a hole on a continuous wave background or on a constant amplitude plane wave. In the case of water waves, the physics is similar but its observation requires special arrangements. Dark solitons can be classified as one of the fundamental waves in nonlinear dynamics in the sense that arbitrary wave configuration can be seen as nonlinear superposition of fundamental modes [4–7]. Clearly, studies in this area of research are important and must be started.

Generally speaking, dark solitons are localized reductions of the amplitude of the envelope field in nonlinear dispersive media [8]. There are a number of equations that admit dark soliton solutions provided the dispersion and nonlinearity are related in a specific way. In particular, the governing equation describing the dynamics of weakly nonlinear and quasi-mono-chromatic waves propagating on the surface of water with arbitrary depth is the nonlinear Schrödinger equation (NLS). Depending on the relative depth h of the water with respect to the wave number of the carrier wave k, the water waves can be described by the NLS either as the focusing or defocusing type. In deep water and more precisely for $kh > 1.363$, the waves are governed by the NLS of the focusing type, which admits a family of stationary bright soliton solution and breathers. These waves have been investigated experimentally in Refs. [9,10] and, more recently, in Ref. [11]. For $kh < 1.363$, the sign of dispersion changes and wave propagation is described by the NLS of the defocusing type which admits dark soliton solutions; they appear as envelope holes [12]. Here, we have to mention that dark solitons may also appear on waters of infinite depth, where the envelope is propagating in two spatial directions [13,14]. Up to now, dark solitons have been observed only in fiber optics [15–17], plasma [18,19], waveguide arrays [20], and Bose-Einstein condensates [21]. In the present work we report the first observation of dark solitons generated in a water wave tank. We also discuss the shape and width of these localized structures which depend on the steepness parameter of the background, its frequency, as well as on the relative water depth.

The NLS describes the space-time evolution of weakly nonlinear wave processes in various dispersive media [22–24]. In the case of water waves, it can be derived by applying the method of multiple scales expansion [25,26]. For arbitrary depth, the equation can be written in the form

$$-i\left(\frac{\partial A}{\partial t} + c_g \frac{\partial A}{\partial x}\right) + \alpha \frac{\partial^2 A}{\partial x^2} + \beta |A|^2 A = 0, \qquad (1)$$

where

$$\alpha = -\frac{1}{2}\frac{\partial^2 \omega}{\partial k^2}$$

is the lowest order dispersion, while

$$\beta = \frac{\omega k^2}{16\sinh^4(kh)}[\cosh(4kh) + 8 - 2\tanh^2(kh)] - \frac{\omega}{2\sinh^2(2kh)}\frac{[2\omega\cosh^2(kh) + kc_g]^2}{gh - c_g^2}$$

is the nonlinear coefficient expressed in terms of the depth h, frequency ω, and wave number k of the carrier wave and the group velocity $c_g = \frac{\partial \omega}{\partial k}$. Independent variables x and t are the space and time coordinates. The dispersion relation of the wave trains on the water surface with finite depth h is

$$\omega = \sqrt{gk\tanh(kh)},$$

where g denotes the gravitational acceleration.

The water surface elevation $\eta(x, t)$ is related to the amplitude $A(x, t)$ in the first order in steepness according to

$$\eta(x, t) = \mathrm{Re}\{A(x, t)\exp[i(kx - \omega t)]\}. \quad (2)$$

In the limit of infinite water depth, that is for the limiting case $kh \to \infty$, the expressions for α and β can be simplified [24]:

$$\alpha = \frac{\omega}{8k^2}, \qquad \beta = \frac{\omega k^2}{2}.$$

For the arbitrary depth case, if $kh > 1.363$, then $\alpha\beta > 0$. In this case, the plane wave solution may be unstable to long-wave perturbations [27,28]. This instability is usually referred to as the Benjamin-Feir instability [24,29,30]. Exact breathing solutions describing this instability have been recently experimentally investigated in Refs. [11,31,32]. Such solutions may also appear naturally from random phase initial conditions provided that the wave spectrum is sufficiently energetic and narrow banded [33,34]. However, for $kh < 1.363$, the nonlinear coefficient β becomes negative and the finite amplitude wave trains in this case are stable. In this work, we conducted experiments to deal with this case.

A scaled form of the NLS in finite depth for $kh < 1.363$ is the well-known defocusing NLS:

$$iq_T + q_{XX} - 2|q|^2 q = 0, \quad (3)$$

which is obtained from (1) by introducing the scaled variables [1]

$$X = x - c_g t, \qquad T = -\alpha t, \qquad q = \sqrt{\frac{-\beta}{2\alpha}}A. \quad (4)$$

Here, X is the coordinate in a frame moving with the group velocity and T is the scaled time. For a given carrier amplitude a, the defocusing NLS admits a one-parameter family of localized soliton solutions, generally known as gray solitons [12,35]. They are described by

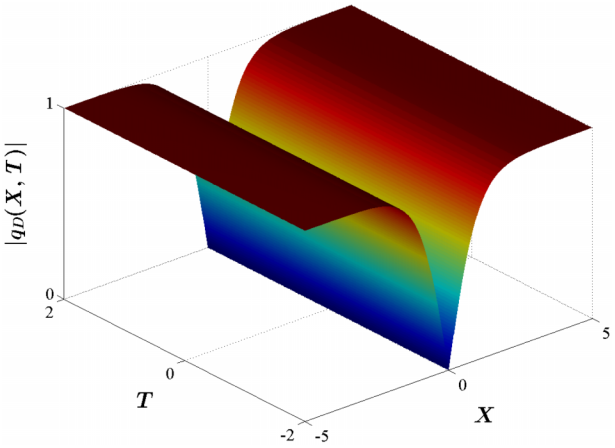

FIG. 1 (color online). Dark soliton solution showing the carrier wave amplitude drop to zero at $X = 0$.

$$q_G = a\frac{\exp(-2im) + \exp[2a(X + 2a\cos(m)T)\sin(m)]}{1 + \exp[2a(X + 2a\cos(m)T)\sin(m)]} \times \exp(-2ia^2T), \quad (5)$$

where m is the parameter of the family that controls the minimal amplitude at the center of the soliton. For $m = \frac{\pi}{2}$, this minimal wave amplitude drops to zero. This limiting case is given by the simpler expression

$$q_D = a\tanh(aX)\exp(-2ia^2T). \quad (6)$$

It is called the black soliton and it is illustrated in Fig. 1 with the value of $a = 1$.

The experiments have been conducted in the wave tank of the Ecole Centrale Marseille/IRPHE. The tank is shown in Fig. 2. It is 17 m long and 0.65 m wide. A single flap-type wave maker is installed at the far end of the tank. An efficient absorbing beach, made with submerged porous plate is installed at the other end. It is clearly visible at the right-hand side of Fig. 2 inside the water with fluorescent dye. The beginning of the beach is located at the distance of 13 m from the wave maker. The vertical walls are made of transparent sections of glass supported by the metal frame. The

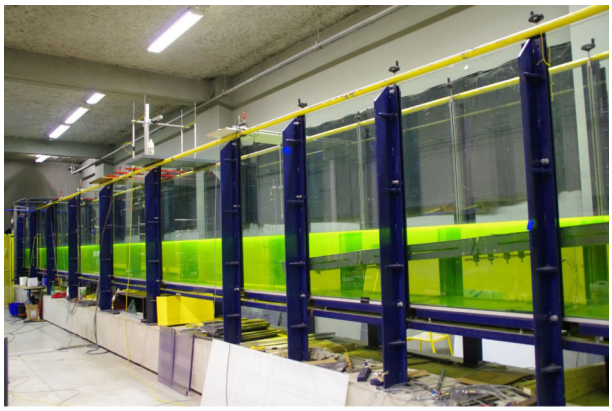

FIG. 2 (color online). Wave channel used in the experiments.

TABLE I. Wave gauge positions.

The gauge number	1	2	3	4	5	6	7
Its position along the tank (m)	1.06	4.33	5.41	7.00	8.86	9.76	12.80

water level of the free surface is measured with seven resistive wave gauges with a sampling frequency of 200 Hz. The location of the gauges is given in Table I.

In order to generate dark solitons, we have to control the flap displacement through the computerized equipment and create initial conditions in dimensional units. This means that Eqs. (6) and (2) have to be dimensionalized with the use of inverted relations (4). Our experiments have been conducted for two different water depth values, $h = 0.40$ and $h = 0.25$ m. In each case, the condition of applicability of the defocusing NLS, i.e., $kh < 1.363$, has been satisfied.

Figure 3 shows the evolution of a black soliton for the carrier amplitude $a = 0.04$ m and the wave number $k = 3\ \mathrm{m}^{-1}$ while the water depth is of $h = 0.40$ m. Each time series has been shifted in time to position the zero of the wave at the same location. As a result, all diagrams are aligned in time for convenience of comparison of their profiles. Moreover, all diagrams are aligned in time by the theoretical value of the group velocity, which is $c_g = 1.18\ \mathrm{m\,s}^{-1}$. Clearly, we observe that the soliton does not change shape and propagates with the corresponding group velocity in accordance with theory since the stationary localizations are almost perfectly aligned in all stages of propagation. In each panel, the experimental curve is supplemented with the envelope calculated using the first-order Fourier analysis. The envelopes are consistent with the theoretical shape of the dark soliton shown in Fig. 1. Another interesting feature of our data is that the difference between the group velocity and the phase velocity leads to a continuous shift of the dark soliton relative to the wave pattern of the carrier. Thus, the phase of the carrier in each of the seven panels is also shifted relative to the previous one.

These data prove that we indeed observed dark solitons. Figure 4 shows similar set of experimental data for the water depth $h = 0.25$ m. Here, the amplitude of the carrier is $a = 0.02$ m while the wave number $k = 4\ \mathrm{m}^{-1}$; thus, the group velocity is $c_g = 1.06\ \mathrm{m\,s}^{-1}$. The alignment of the bump, which is located at zero amplitude level in both experiments, show that the theoretical value of the group velocity is again in accordance with the theoretical value and this is another proof that we are dealing with the dark soliton although with the parameters of the experiment different from the previous case.

A video showing the dynamics of surface elevation in the flume can be found in the Supplemental Material [36]. The video demonstrates clearly the decrease of the amplitude near zero point of the dark soliton profile.

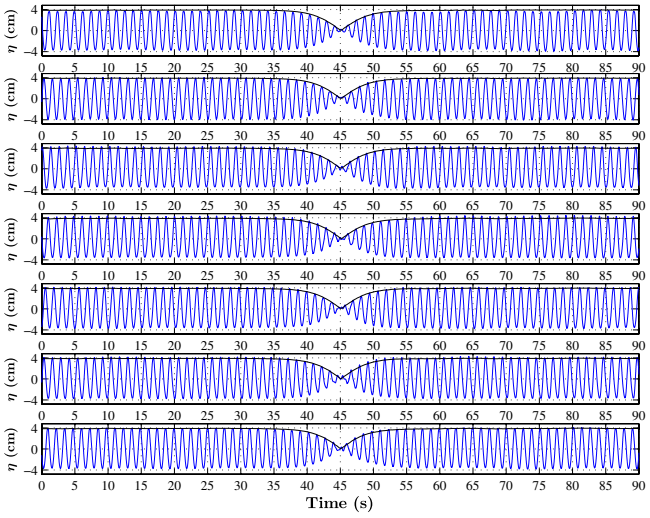

FIG. 3 (color online). Evolution of the dark soliton along the tank with the water depth $h = 0.4$ m. The carrier amplitude is $a = 0.04$ m, while $kh = 1.2$. Seven panels from top to bottom correspond to experimental records of seven gauges from 1 to 7, respectively, shifted in time to keep zero amplitude at the same position. The envelope over the experimental curves computed using the first-order Fourier analysis is in good agreement with theoretical dark soliton shape.

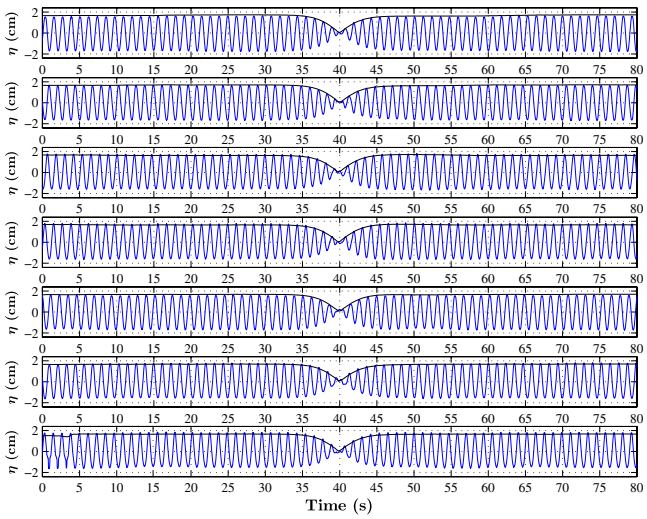

FIG. 4 (color online). Evolution of the dark soliton along the tank with the water depth $h = 0.25$ m. The carrier amplitude is $a = 0.02$ m, while $kh = 1.0$. Seven panels from top to bottom correspond to experimental records of seven gauges from 1 to 7, respectively, shifted in time to keep zero amplitude at the same position. The envelope over the experimental curves computed using the first-order Fourier analysis is in good agreement with theoretical dark soliton shape.

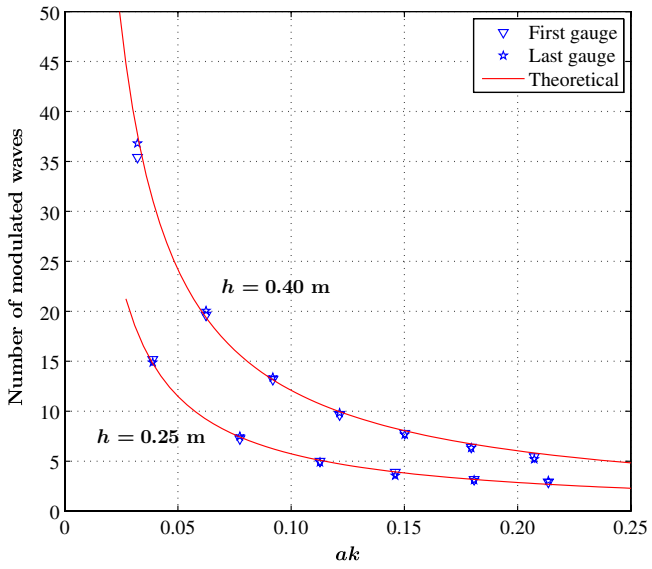

FIG. 5 (color online). The number of modulated waves within the dark soltion versus steepness ak. The former is defined with the threshold amplitude of $0.9a$ for the corresponding depth. The triangles correspond the values obtained from the first gauge. The stars correspond the values obtained from the last gauge. Solid lines are obtained from theoretical calculations.

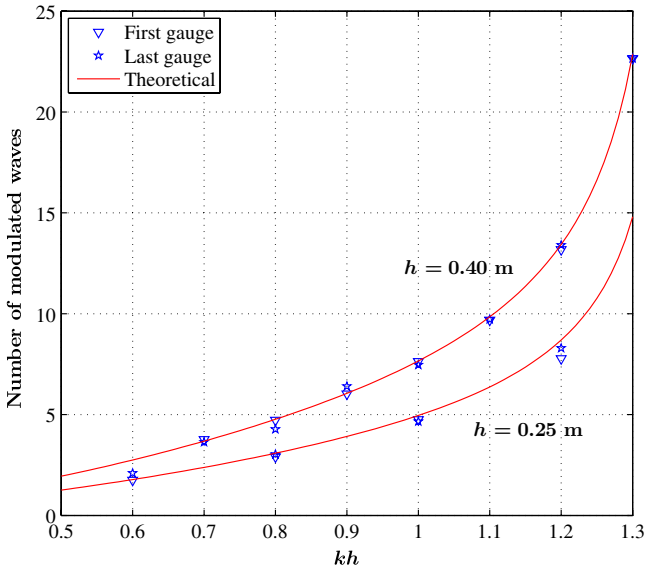

FIG. 6 (color online). The number of modulated waves within the soliton versus kh. The former is defined for the threshold amplitude $0.9a$ for the corresponding depth. The triangles correspond the values obtained from the first gauge. The stars correspond the values obtained from the last gauge. Solid lines are obtained from theoretical calculations.

Further verification that it is the dark soliton excited on the surface of water can be obtained from confirming its effective width. In order to do that we calculated the number of carrier waves within the soliton, i.e., the number of waves with modulated amplitude versus the steepness of the background wave. We estimated this dependence from our experimental data by defining the modulated waves as those whose amplitude is less than 0.9 of the carrier amplitude. Then, we calculated the number of modulated waves defined this way within the soliton. Fractional values can be obtained if we best fit the envelope through the wave maxima. Figure 5 shows these data for the first and the last gauges for the two h values as a function of the steepness ak. The data for all other gauges are very similar to these. Theoretical curves shown by the solid lines demonstrate that the number of modulated waves is inversely proportional to the steepness of the background. Comparison of experimental data with the theoretical curves proves once again that we do observe dark solitons.

The number of modulated waves within the dark soliton depends also on the wave number k for fixed h. We calculated the number of modulated waves the same way as described above for several values of k. Figure 6 shows these data for the two values of the depth h along with the theoretical curves. The plot shows that our observations fit well the theoretical relationship between the number of modulated waves and the combined parameter kh.

To conclude, our experimental study proves the existence of dark solitons in water waves. Our observations of these localized structures are in agreement with the theoretical prediction: the solitons preserve fixed shape during their evolution in the tank. Furthermore, the solitons propagate exactly with the group velocity for the corresponding wave number, wave frequency and water depth calculated theoretically. Generally, these results confirm that the NLS equation provides a good description of surface gravity waves even in the defocusing case. Thus, water waves have to be described in the frame of nonlinear dynamics rather than just a linear superposition of modes.

A. C. would like to thank Roger Grimshaw and Efim Pelinovsky for helpful discussions. N. H. and N. A. acknowledge the support of the Volkswagen Stiftung. N. A. acknowledges partial support of the Australian Research Council (Discovery Project No. DP110102068). N. A. acknowledges support from the Alexander von Humboldt Foundation. M. O. was supported by EU, project EXTREME SEAS (SCP8-GA-2009-234175) and ONR Grant No. N000141010991. M. O. acknowledges Dr. B. Giulinico for interesting discussions.

*a.chabchoub@imperial.ac.uk

[1] A. Osborne, *Nonlinear Ocean Waves and the Inverse Scattering Transform* (Elsevier, Amsterdam, 2010).
[2] D. R. Solli, C. Ropers, P. Koonath, and B. Jalali, Nature (London) **450**, 1054 (2007).
[3] N. Akhmediev and E. Pelinovsky, Eur. Phys. J. Special Topics **185** 1 (2010).
[4] *Solitary Waves in Fluids*, edited by R. H. J. Grimshaw (WIT, Southampton, Boston, 2007).

[5] C. Kharif, E. Pelinovsky, and A. Slunyaev, *Rogue Waves in the Ocean* (Springer, Heidelberg, NY, 2009).
[6] D. E. Pelinovsky, Y. S. Kivshar, and V. V. Afanasjev, Phys. Rev. E **54**, 2015 (1996).
[7] M. J. Ablowitz, *Nonlinear Dispersive Waves* (Cambridge University Press, Cambridge, England, 2011).
[8] Y. S. Kivshar and B. Luther-Davies, Phys. Rep. **298**, 81 (1998).
[9] H. C. Yuen and B. M. Lake, Phys. Fluids **18**, 956 (1975).
[10] H. C. Yuen and B. M. Lake, Adv. Appl. Mech. **22**, 67 (1982).
[11] A. Chabchoub, N. P. Hoffmann, and N. Akhmediev, Phys. Rev. Lett. **106**, 204502 (2011).
[12] D. H. Peregrine, J. Aust. Math. Soc. Series B, Appl. Math. **25**, 16 (1983).
[13] W. H. Hui and J. Hamilton, J. Fluid Mech. **93**, 117 (1979).
[14] F. Baronio, A. Degasperis, M. Conforti, and S. Wabnitz, Phys. Rev. Lett. **109**, 044102 (2012).
[15] P. Emplit, J. P. Hamaide, F. Reynaud, C. Froehly, and A. Barthelemy, Opt. Commun. **62**, 374 (1987).
[16] D. Krökel, N. J. Halas, G. Giuliani, and D. Grischkowsky, Phys. Rev. Lett. **60**, 29 (1988).
[17] A. M. Weiner, J. P. Heritage, R. J. Hawkins, R. N. Thurston, E. M. Kirschner, D. E. Leaird, and W. J. Tomlinson, Phys. Rev. Lett. **61**, 2445 (1988).
[18] P. K. Shukla and B. Eliasson, Phys. Rev. Lett. **96**, 245001 (2006).
[19] R. Heidemann, S. Zhdanov, R. Sütterlin, H. M. Thomas, and G. E. Morfill, Phys. Rev. Lett. **102**, 135002 (2009).
[20] E. Smirnov, C. E. Rüter, M. Stepić, D. Kip, and V. Shandarov, Phys. Rev. E **74**, 065601(R) (2006).
[21] D. J. Frantzeskakis, J. Phys. A **43**, 213001 (2010).
[22] R. Y. Chiao, E. Garmire, and C. H. Towns, Phys. Rev. Lett. **13**, 479 (1964).
[23] D. J. Benney and A. C. Newell, J. Math. Phys. (N.Y.) **46**, 133 (1967).
[24] V. E. Zakharov, J. Appl. Mech. Tech. Phys. **9**, 190 (1968).
[25] H. Hasimoto and H. Ono, J. Phys. Soc. Jpn. **33**, 805 (1972).
[26] C. C. Mei, *The Applied Dynamics of Ocean Surface Waves*, Advanced Series on Ocean Engineering Vol. 1 (World Scientific, Singapore, 1983).
[27] A. Newell, *Solitons in Mathematics and Physics* (Society for Industrial and Applied Mathematics, Philadelphia, 1985).
[28] F. Dias and C. Kharif, Annu. Rev. Fluid Mech. **31**, 301 (1999).
[29] M. J. Lighthill, J. Inst. Math. Appl. **1**, 269 (1965).
[30] T. B. Benjamin and J. E. Feir, J. Fluid Mech. **27**, 417 (1967).
[31] G. F. Clauss, M. Klein, and M. Onorato, *Proceedings of the ASME 2011 30th International Conference on Ocean, Offshore and Arctic Engineering OMAE2011, Rotterdam, The Netherlands, 2011* (ASME, New York, 2011), pp. 417–429.
[32] A. Chabchoub, N. Hoffmann, M. Onorato, and N. Akhmediev, Phys. Rev. X **2**, 011015 (2012).
[33] M. Onorato, A. R. Osborne, M. Serio, and S. Bertone, Phys. Rev. Lett. **86**, 5831 (2001).
[34] M. Onorato, A. R. Osborne, R. Fedele, and M. Serio, Phys. Rev. E **67**, 046305 (2003).
[35] V. E. Zakharov and A. B. Shabat, Zh. Eksp. Teor. Fiz. **64**, 1627 (1973) [Sov. Phys. JETP **37**, 823 (1973)].
[36] See Supplemental Material at http://link.aps.org/supplemental/10.1103/PhysRevLett.110.124101 for the experimental demonstration of the generation of a black soliton in a wave flume. The video demonstrates clearly the decrease of the amplitude near zero point of the dark soliton profile.